Electronic Supplementary Material (ESI) for RSC Advances.
This journal is © The Royal Society of Chemistry 2015

Supporting Information for

Luminescence and slow magnetic relaxation of 2D isostructural lanthanide metal-organic frameworks based on nicotinate *N*-oxide and glutarate

Cai-Ming Liu,* De-Qing Zhang, Xiang Hao and Dao-Ben Zhu
Beijing National Laboratory for Molecular Sciences, Center for Molecular Science, Key Laboratory of Organic Solids，Institute of Chemistry, Chinese Academy of Sciences, Beijing 100190, P.R. China

Table S1. Continuous Shape Measures calculation for the Dy(III) ion in **3**.

Dy1, nine-coordination

Dy1	EP-9	OPY-9	HBPY-9	JTC-9	JCCU-9	CCU-9	JCSAPR-9	CSAPR-9	JTCTPR-9	TCTPR-9	JTDIC-9	HH-9	MFF-9
ABOXIY	34.281	22.378	18.215	15.355	10.519	10.333	2.177	1.913	3.800	2.703	13.475	9.994	1.711

EP-9	1	D9h	Enneagon
OPY-9	2	C8v	Octagonal pyramid
HBPY-9	3	D7h	Heptagonal bipyramid
JTC-9	4	C3v	Johnson triangular cupola J3
JCCU-9	5	C4v	Capped cube J8
CCU-9	6	C4v	Spherical-relaxed capped cube
JCSAPR-9	7	C4v	Capped square antiprism J10
CSAPR-9	8	C4v	Spherical capped square antiprism
JTCTPR-9	9	D3h	Tricapped trigonal prism J51
TCTPR-9	10	D3h	Spherical tricapped trigonal prism
JTDIC-9	11	C3v	Tridiminished icosahedron J63
HH-9	12	C2v	Hula-hoop

MFF-9	13	Cs	Muffin

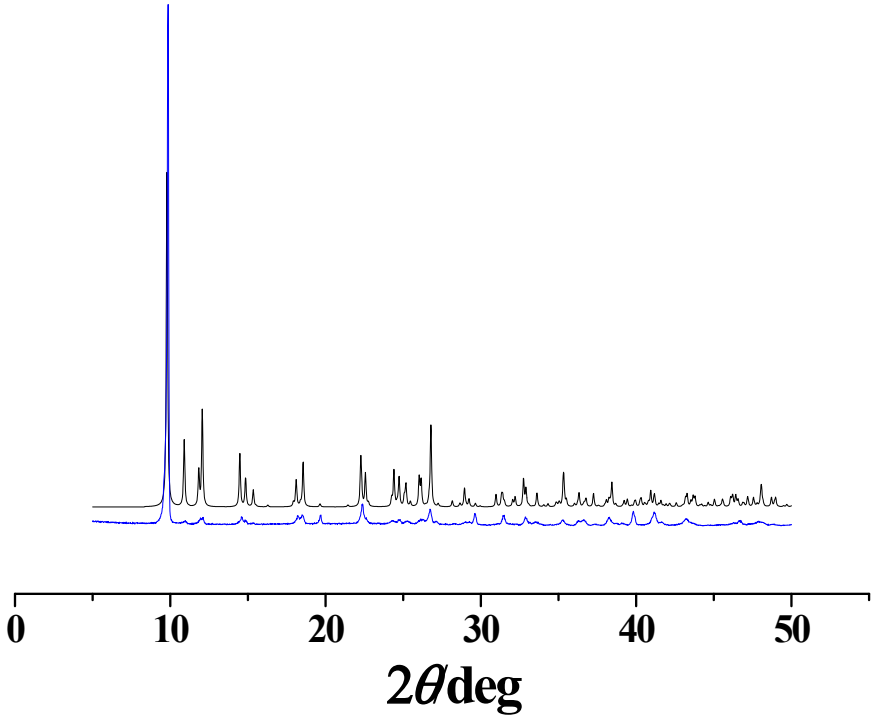

Fig. S1. The simulative (black) and experimental (blue) powder X-ray diffraction patterns for **1**.

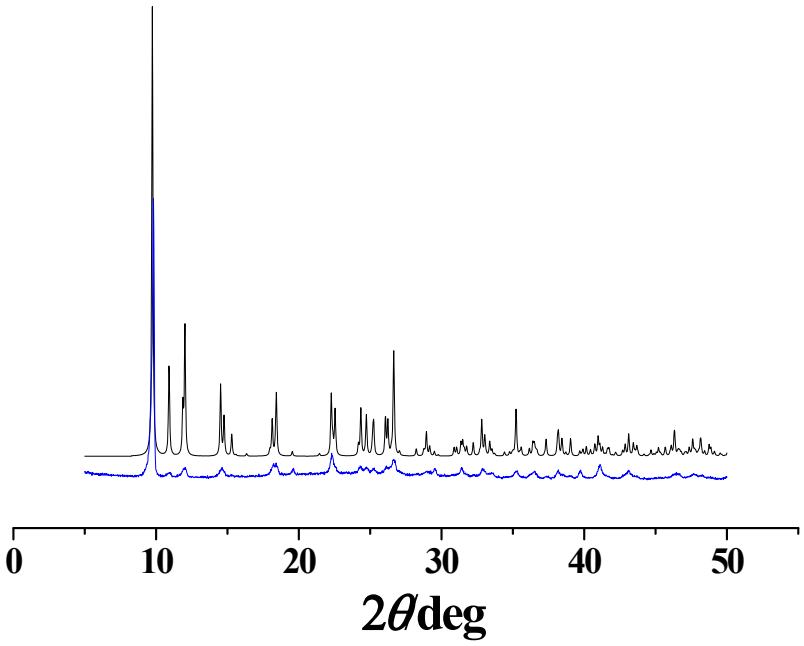

Fig. S2. The simulative (black) and experimental (blue) powder X-ray diffraction patterns for **2**.

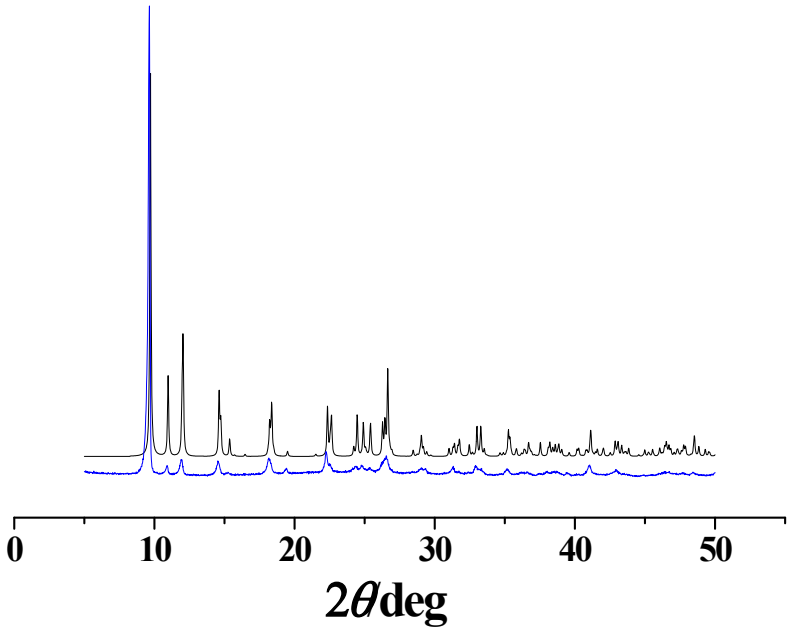

Fig. S3. The simulative (black) and experimental (blue) powder X-ray diffraction patterns for **3**.

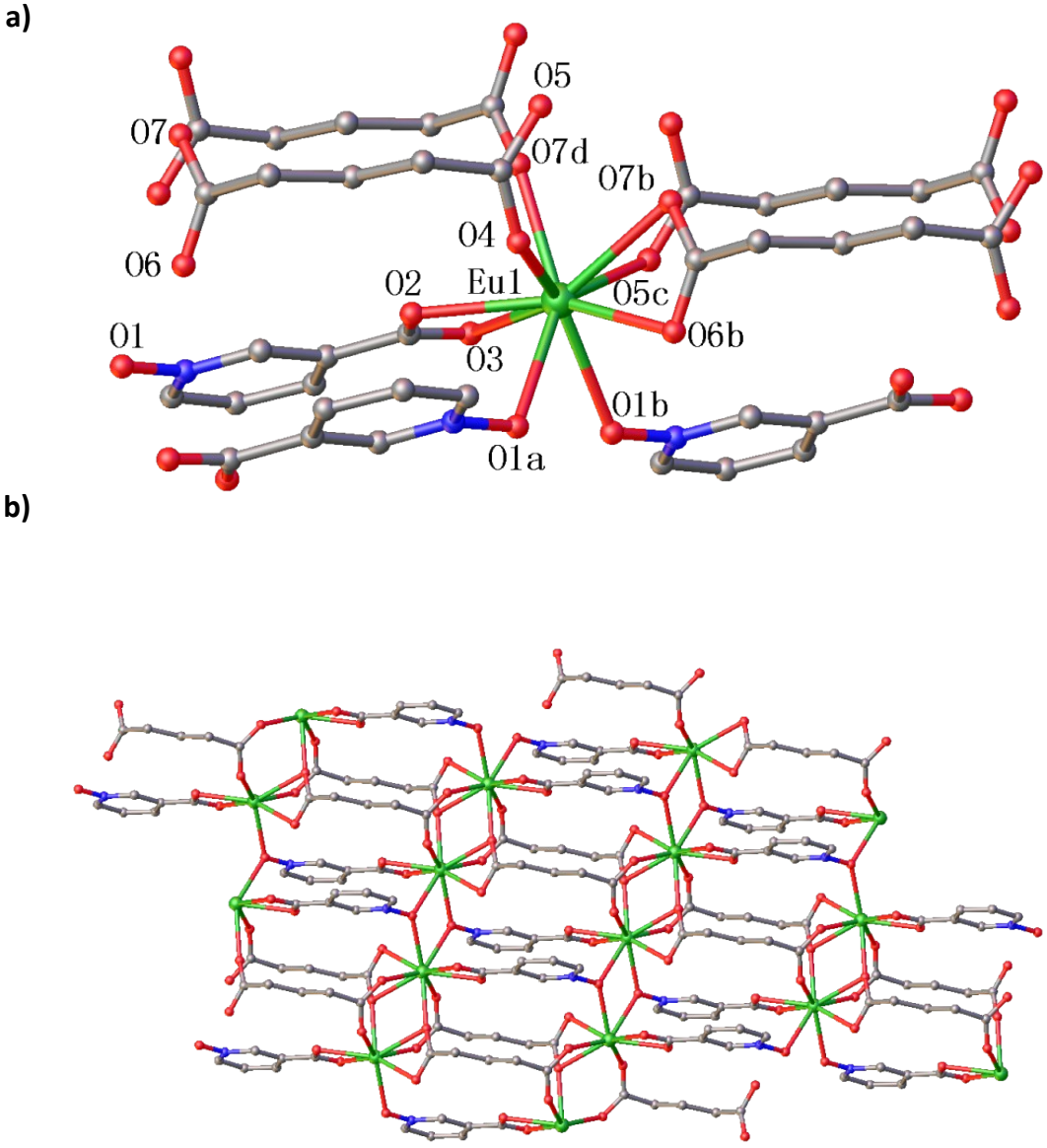

Fig. S4. The coordination environments of the Eu atom in **1** (a), symmetry codes: a: 1/2−x, −1/2−y, 1−z; b: 1/2+x, 1/2+y, z; c: 1/2−x, 1/2−y, 1−z; d: −x, −y, 1−z; and 2D layer structure of **1** viewed down the *c*-axis (b).

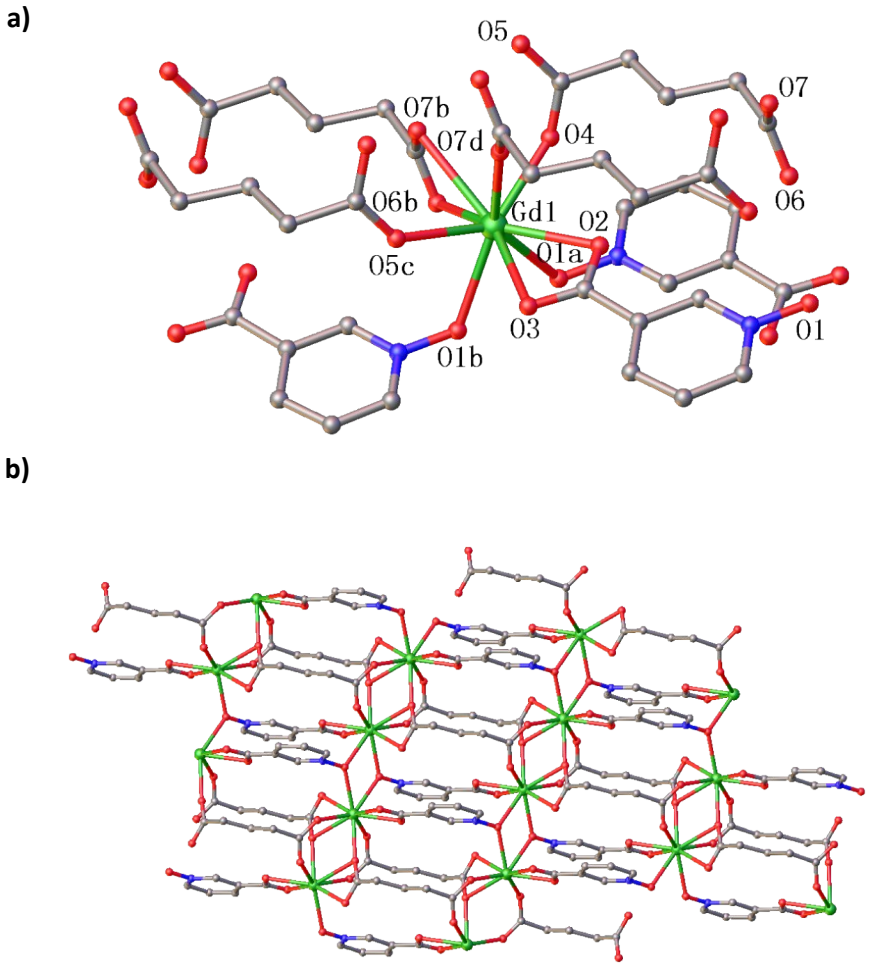

Fig. S5. The coordination environments of the Gd atom in **2** (a), symmetry codes: a: 1/2−x, −1/2−y, 1−z; b: 1/2+x, 1/2+y, z; c: 1/2−x, 1/2−y, 1−z; d: −x, −y, 1−z; and 2D layer structure of **2** viewed down the *c*-axis (b).

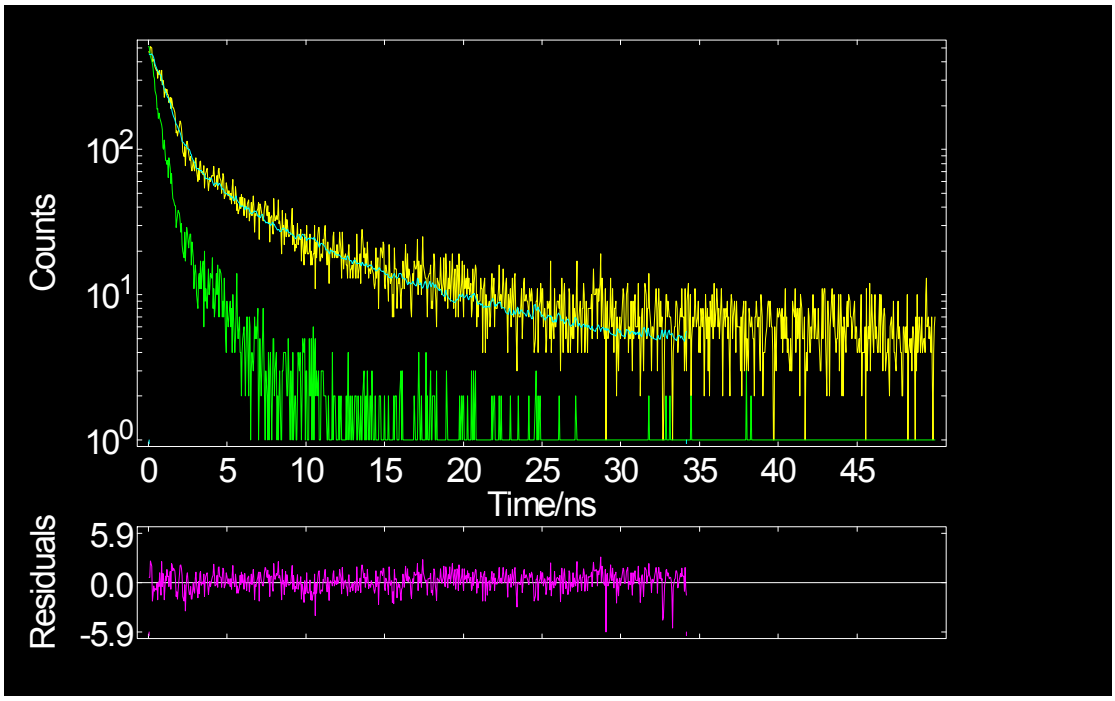

Fig. S6. $^5D_0$ decay and fitted curves of complex **1** measured at room temperature. Emission was monitored at 615 nm and the excitation was performed at 400 nm.

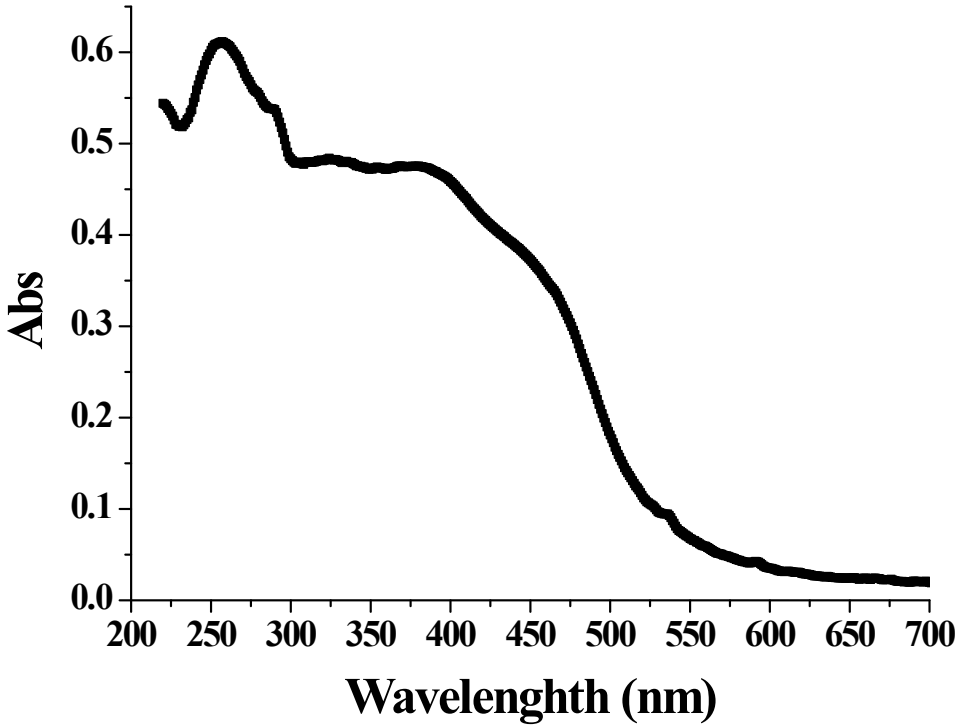

Fig. S7. The absorption spectrum of the microcrystalline solids of compound **1** measured with an integrated sphere.

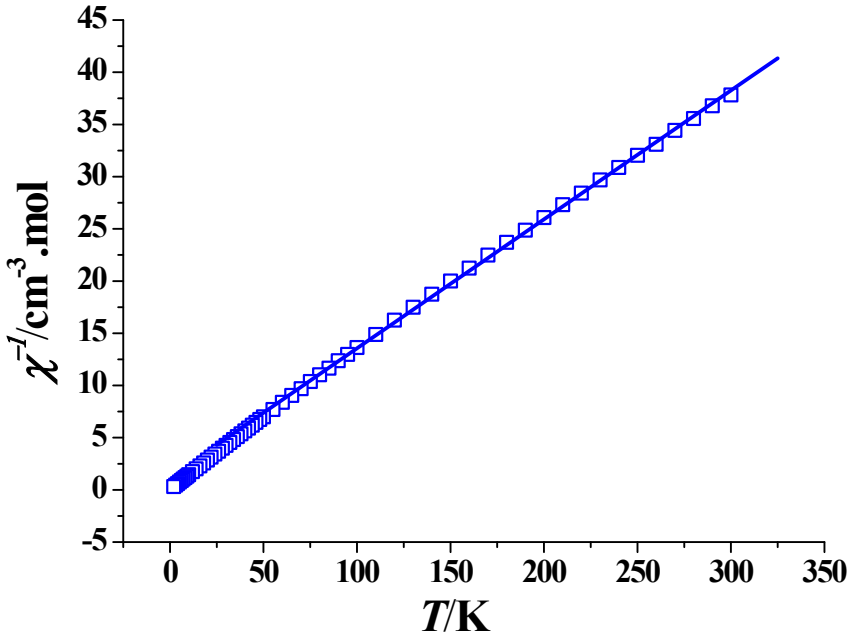

Fig. S8. $1/\chi$ versus T of **2**, the solid line represents the best theoretical fitting.

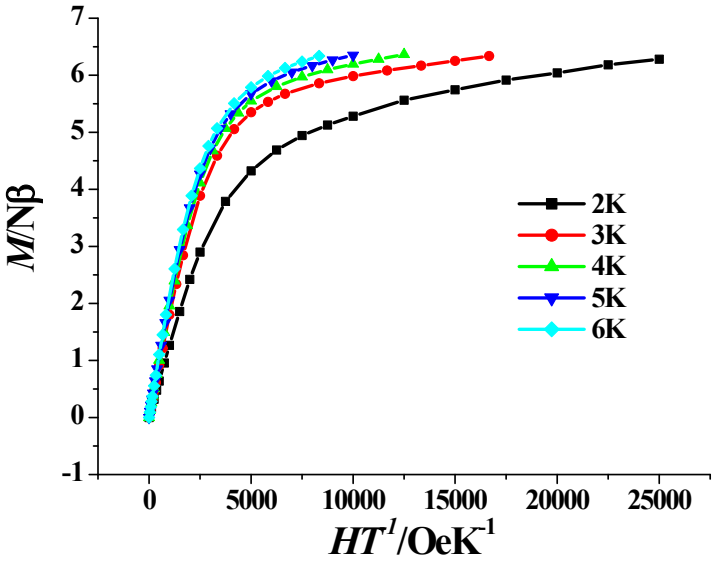

Fig. S9. M versus H/T plots at 2–6 K of **3**.

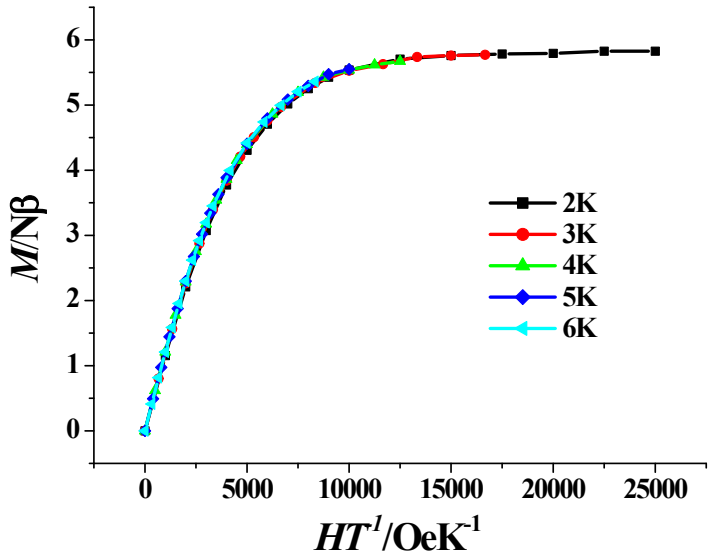

Fig. S10. *M* versus *H*/*T* plots at 2–6 K of **2**.

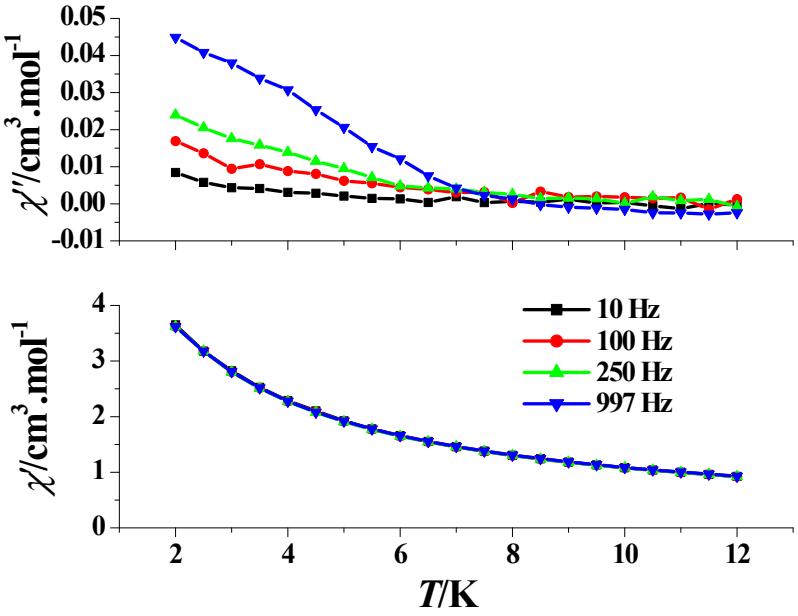

Fig. S11. AC susceptibilities measured in a 2.5 Oe ac magnetic field with a zero dc field for **3.**

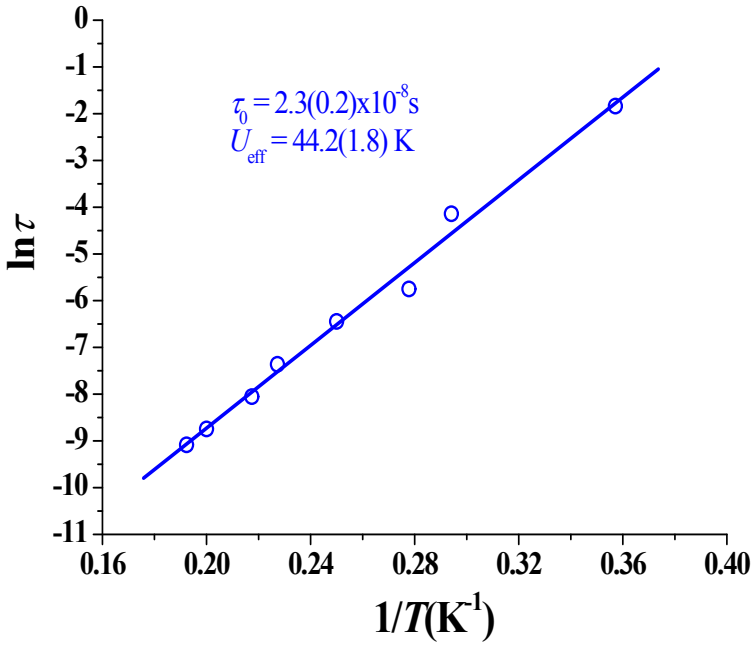

Fig. S12. Plot of ln(τ) versus $1/T_B$ for **3,** the solid lines represent the best fitting with the Arrhénius law.

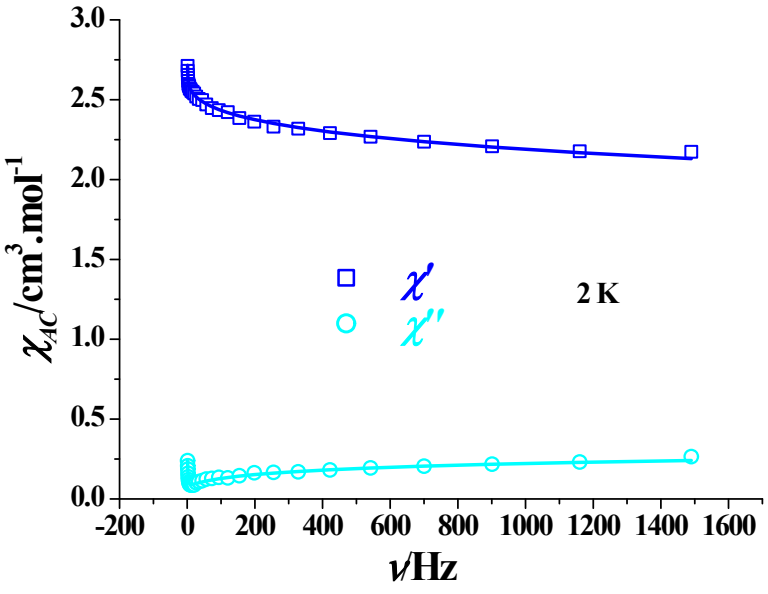

Fig. S13. Frequency dependence of the in-phase (χ', top) and out-of-phase (χ'', bottom) ac susceptibility of **3** at 2 K. the solid lines represent the best fitting with the sum of two modified Debye functions

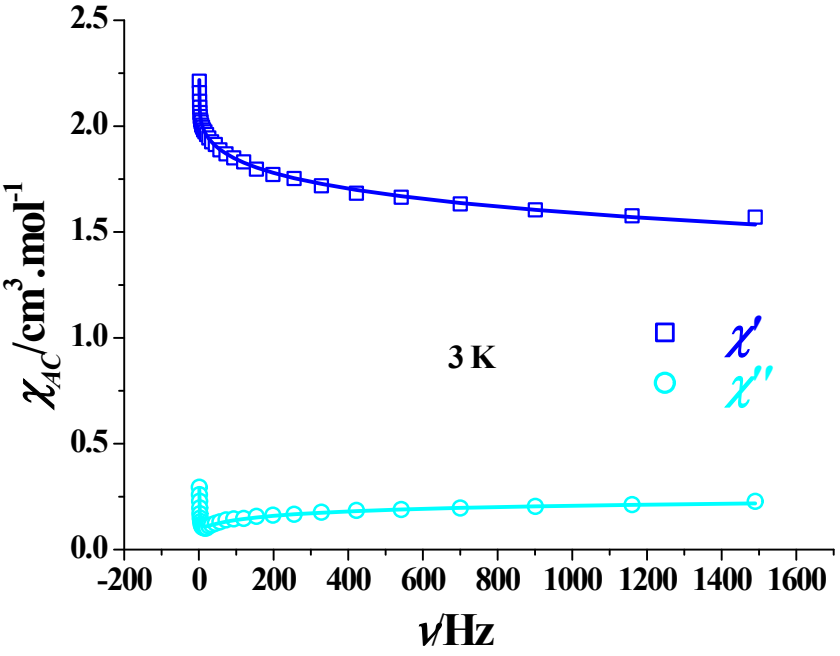

Fig. S14. Frequency dependence of the in-phase (χ', top) and out-of-phase (χ'', bottom) ac susceptibility of **3** at 3 K. the solid lines represent the best fitting with the sum of two modified Debye functions.

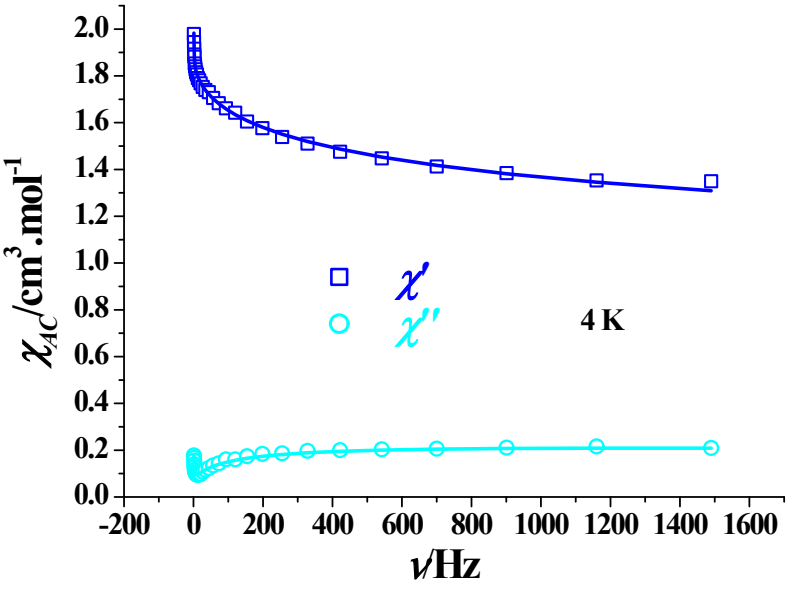

Fig. S15. Frequency dependence of the in-phase (χ', top) and out-of-phase (χ'', bottom) ac susceptibility of **3** at 4 K. the solid lines represent the best fitting with the sum of two modified Debye functions.

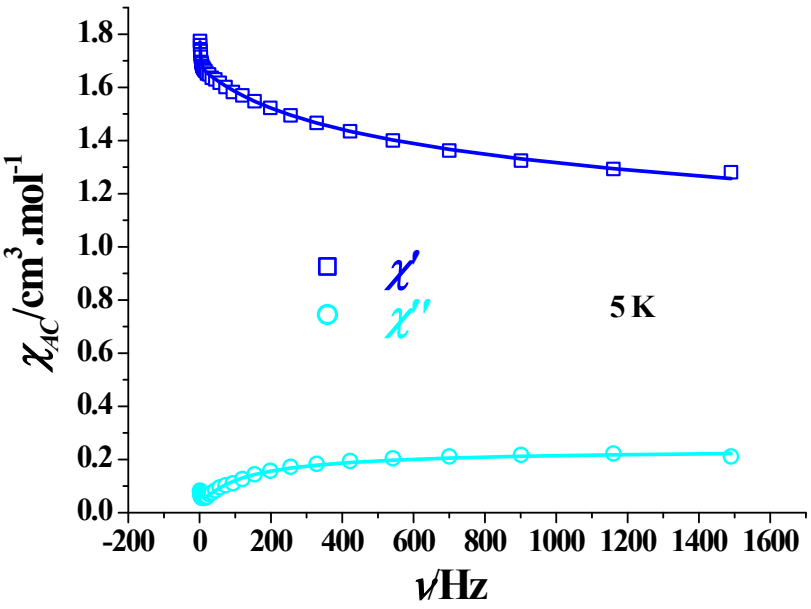

Fig. S16. Frequency dependence of the in-phase (χ', top) and out-of-phase (χ'', bottom) ac susceptibility of **3** at 5 K. the solid lines represent the best fitting with the sum of two modified Debye functions.

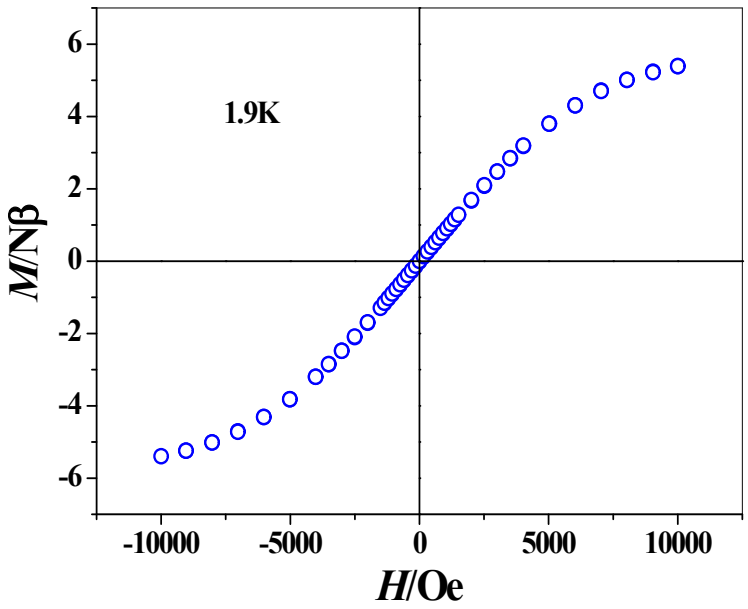

Fig. S17. Plot of M versus H at 1.9 K from −10000 to 10000 Oe for **3**.

Table S2. Linear combination of two modified Debye model fitting parameters from 2 K to 5 K of **3** under 2k Oe dc field.

T(K)	χ_2(cm^3.mol^{-1})	χ_1(cm^3.mol^{-1})	χ_0(cm^3.mol^{-1})	τ_1(s)	α_1	τ_2(s)	α_2
2	2.67585	3.34404	1.9481E-6	2.3645E-6	0.66397	0.43354	0.03787
3	2.73233	2.1514	0.18875	0.00001	0.68175	0.27605	0.00023
4	2.22941	1.9002	0.76017	0.00012	0.55338	0.21776	0.0284
5	2.06077	0.00061	2.49173	0.00009	0.71095	0.0061	0.1069